

Tunnel electroresistance in junctions with ultrathin ferroelectric Pb(Zr_{0.2}Ti_{0.8})O₃ barriers

Daniel Pantel, Haidong Lu, Silvana Goetze, Peter Werner, Dong Jik Kim et al.

Citation: *Appl. Phys. Lett.* **100**, 232902 (2012); doi: 10.1063/1.4726120

View online: <http://dx.doi.org/10.1063/1.4726120>

View Table of Contents: <http://apl.aip.org/resource/1/APPLAB/v100/i23>

Published by the [American Institute of Physics](http://www.aip.org).

Related Articles

Polarization and interface charge coupling in ferroelectric/AlGaIn/GaN heterostructure

Appl. Phys. Lett. **100**, 112902 (2012)

Ultrahigh dielectric constant of thin films obtained by electrostatic force microscopy and artificial neural networks

Appl. Phys. Lett. **100**, 023101 (2012)

Converse-piezoelectric effect on current-voltage characteristics of symmetric ferroelectric tunnel junctions

J. Appl. Phys. **111**, 014103 (2012)

Ferroelectric and electrical characterization of multiferroic BiFeO₃ at the single nanoparticle level

Appl. Phys. Lett. **99**, 252905 (2011)

Defect enhanced optic and electro-optic properties of lead zirconate titanate thin films

AIP Advances **1**, 042144 (2011)

Additional information on *Appl. Phys. Lett.*

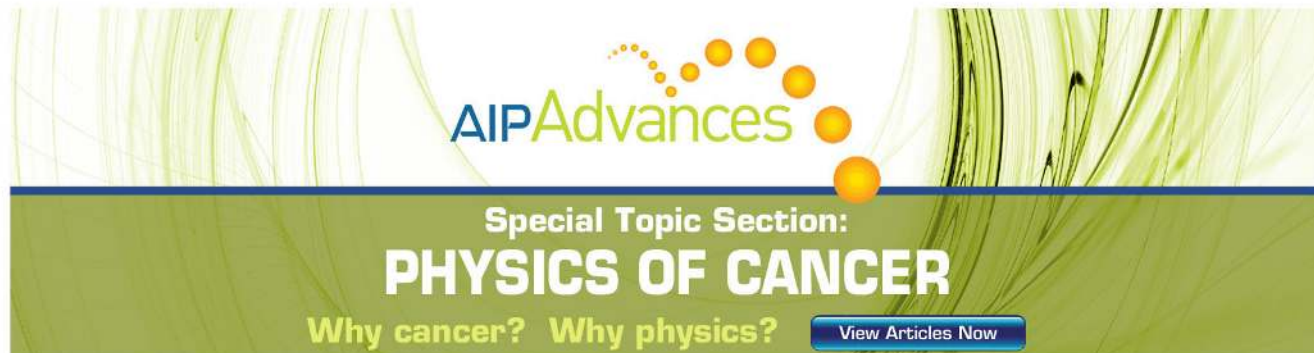
Journal Homepage: <http://apl.aip.org/>

Journal Information: http://apl.aip.org/about/about_the_journal

Top downloads: http://apl.aip.org/features/most_downloaded

Information for Authors: <http://apl.aip.org/authors>

ADVERTISEMENT



AIP Advances

Special Topic Section:
PHYSICS OF CANCER

Why cancer? Why physics? [View Articles Now](#)

Tunnel electroresistance in junctions with ultrathin ferroelectric $\text{Pb}(\text{Zr}_{0.2}\text{Ti}_{0.8})\text{O}_3$ barriers

Daniel Pantel,¹ Haidong Lu,² Silvana Goetze,¹ Peter Werner,¹ Dong Jik Kim,² Alexei Gruverman,² Dietrich Hesse,¹ and Marin Alexe^{1,a)}

¹Max Planck Institute of Microstructure Physics, Weinberg 2, 06120 Halle, Germany

²University of Nebraska, Lincoln, Nebraska 68588, USA

(Received 11 April 2012; accepted 19 May 2012; published online 5 June 2012)

In ferroelectric tunnel junctions, the ferroelectric polarization state of the barrier influences the quantum-mechanical tunneling through the junction, resulting in tunnel electroresistance (TER). Here, we investigate tunnel electroresistance in $\text{Co}/\text{PbZr}_{0.2}\text{Ti}_{0.8}\text{O}_3/\text{La}_{0.7}\text{Sr}_{0.3}\text{MnO}_3$ tunnel junctions. The ferroelectric polarization in tunnel junctions with 1.2-1.6 nm (three to four unit cells) $\text{PbZr}_{0.2}\text{Ti}_{0.8}\text{O}_3$ thickness and an area of $0.04 \mu\text{m}^2$ can be switched by about 1 V yielding a resistive ON/OFF-ratio of about 300 at 0.4 V. Combined piezoresponse force microscopy and electronic transport investigations of these junctions reveal that the transport mechanism is quantum tunneling and the resistive switching in these junctions is due only to ferroelectric switching. © 2012 American Institute of Physics. [<http://dx.doi.org/10.1063/1.4726120>]

The ferroelectric polarization state in a metal/ferroelectric/metal heterostructure is usually read by detecting the switched charge generated by a voltage pulse applied to the heterostructures.¹ This approach is currently used in ferroelectric random access memories with the obvious disadvantage of a destructive read-out process. Thus, reading the ferroelectric state in a non-destructive manner using a polarization-coupled physical property, for instance, the electric resistance,² would be advantageous. The change in the resistance upon the ferroelectric polarization reversal is called ferroelectric electroresistance effect. Since the polarization can be switched by a short voltage pulse, this might be regarded as a genuine electronic resistive switching effect.

Resistive switching in ferroelectrics has already been reported several times.³⁻¹² However, there are mechanisms other than ferroelectric polarization switching, which might contribute to or generate a resistive switching effect, such as, for instance, surface electrochemical reactions.^{4,13} Especially, experiments performed in ambient conditions by using a conductive atomic force microscope (AFM) tip in contact with a ferroelectric surface are prone to such effects.¹⁴ Up to now, most of the measurements performed on ferroelectric barriers with thicknesses small enough to allow direct quantum-mechanical tunneling have been performed by such a method.^{5,6,10}

In order to mitigate the spurious effects of the ambient environment and make the experimental results more reliable, capacitor-like heterostructures with top electrodes should be used instead of AFM tips as top electrodes. Resistive switching of such capacitors with relatively thick $\text{Pb}(\text{Zr,Ti})\text{O}_3$ (PZT) barriers (ca. 9 nm) has already been performed.⁷ In these studies, Schottky emission was suggested as the dominating transport mechanism. For smaller barrier thickness, direct tunneling should be the dominant transport

mechanism, as predicted by theoretical simulations.¹⁵ Because of this feature, these structures are typically referred to as ferroelectric tunnel junctions (FTJ).¹⁶ Although electroresistance is lower for direct tunneling as compared to Schottky emission, the current density is higher,¹⁵ which is an important parameter for prospective applications. Furthermore, FTJs allow a combination of tunnel electroresistance (TER) effect with the tunnel magnetoresistance (TMR) effect, which can lead to interesting magnetoelectric effects and memory devices with four states.¹⁷⁻²¹ One of the challenges in realization of functional FTJs is a necessity to directly correlate the change in resistance with polarization reversal,^{4,11} which would provide an unambiguous proof of the genuine electronic nature of resistive switching in the ferroelectric barrier.

Here, we combine piezoresponse force microscopy measurements (PFM) and electronic transport investigations by means of conductive AFM on $\text{Co}/\text{PbZr}_{0.2}\text{Ti}_{0.8}\text{O}_3/\text{La}_{0.7}\text{Sr}_{0.3}\text{MnO}_3$ (Co/PZT/LSMO) tunnel junctions with the PZT barrier thickness of three to four unit cells. We present the evidence of the ferroelectric (electronic) origin of TER in these heterostructures, which is significantly larger as compared to BaTiO (BTO)-based FTJs.²²

PZT/LSMO oxide heterostructures were epitaxially and fully coherently grown by pulsed laser deposition on (100)-oriented SrTiO_3 substrates at elevated temperatures. Polycrystalline Au/Co top electrodes were deposited *ex-situ* by thermal evaporation at room temperature. Nanosphere lithography was used to fabricate triangular shaped tunnel junctions with an area of $0.04 \mu\text{m}^2$.⁷ A transmission electron microscope (TEM) image of a tunnel junction is shown in Fig. 1. Details of the growth and fabrication process can be found elsewhere.⁷ In particular, structural and electrical quality of the LSMO and PZT layers used in the present study are similar to those used in Ref. 7. The LSMO layers show good metallic conduction behavior at room temperature yielding an estimated serial resistance of the bottom electrode of about 800Ω , which is far below the typical

^{a)}Author to whom correspondence should be addressed. Electronic mail: malixe@mpi-halle.de.

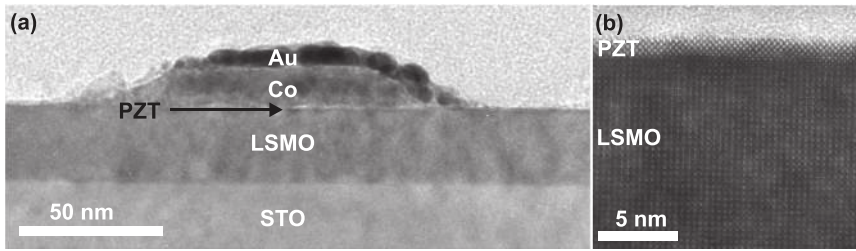


FIG. 1. (a) TEM image of a Co/PZT(3 to 4 unit cells)/LSMO tunnel junction grown on STO. The Co is capped by a gold-layer to prevent oxidation. (b) High resolution TEM image showing the epitaxial PZT/LSMO interface of the same sample in a region without Co top electrode.

resistance of a $0.04 \mu\text{m}^2$ tunnel junction. Thicker PZT layers grown at the same growth conditions show a spontaneous polarization of about $110 \mu\text{C}/\text{cm}^2$ and an excellent retention,⁷ as expected for PZT films free from extended defects.²³

Due to the low PFM-signal of the ultrathin PZT barriers, PFM was performed in the dual ac resonance tracking mode²⁴ using a MFP-3DTM AFM microscope (Asylum Research) and platinum coated tips (DPER18, MikroMasch). Ferroelectric properties of the PZT layers at room temperature were measured by obtaining PFM hysteresis loops with an ac modulation voltage amplitude of 0.3 V. *IV*-curves have been recorded with a conductive diamond coated tip (CDT-NCHR, NanoWorld) and setting the current limit of the current amplifier to 20 nA. The voltage was applied to the bottom electrode and contact was made through the conduc-

tive tip to the top electrode for both measurement methods as depicted in the inset of Fig. 2(a).

Figure 2(a) shows the typical PFM hysteresis loops measured in Co/PZT/LSMO tunnel junctions. The coercive voltages vary from junction to junction and are on average $+0.8 \pm 0.5$ V and -1.4 ± 0.5 V. This alone is an interesting result, as it demonstrates switchable ferroelectric polarization at room temperature in the PZT layers of only three to four unit cell thickness, which is close to the theoretical value of the critical thickness for ferroelectric PbTiO_3 (1.2 nm (Ref. 25)), the parent compound of present PZT. The average coercive field $E_c = 690 \text{ kV}/\text{mm}$ is about three times larger than that of the 9 nm thick PZT layer,⁷ which is in agreement with the known thickness dependence of E_c in ferroelectric films.²⁶

The resistive state of the FTJs can be switched from high conducting (ON-state) to low conducting (OFF-state) and *vice versa* by sweeping the voltage from negative to positive and back, respectively (Fig. 2(a)). The OFF/ON resistance ratio $R_{\text{OFF}}/R_{\text{ON}}$ is approximately 300 at 0.4 V. Resistive switching occurs here on average at $+0.7 \pm 0.2$ V from ON to OFF and at -1.7 ± 0.2 V from OFF to ON. Thus, the switching voltages of ferroelectric switching and resistive switching coincide within the experimental errors confirming that the resistive switching is only due to polarization switching. The junction is in ON- or OFF-state for polarization pointing towards LSMO or Co, respectively. The resistive switching in ferroelectric tunnel junctions can be explained by assuming a simple electrostatic model of a ferroelectric tunnel barrier that considers the effective screening lengths,^{15,21} which is larger for LSMO than for the Co electrode.^{27,28}

The resistance area product (*RA*) of the junctions is about $6 \text{ M}\Omega\mu\text{m}^2$ in the ON-state (measured at 100 mV), which is in the typical range for tunnel junctions.²⁹ More insight into the transport mechanism can be gained from the tunnel conductance $G = dI/dV$ calculated from the *IV*-characteristics. The $G(V)$ -curve is parabola-like (Fig. 2(b)) as expected for transport-dominating direct tunneling.³⁰ It can be fit to the Brinkman model³⁰ for a fixed PZT thickness d yielding reasonable fit parameters for barrier heights Φ_i ($i = 1,2$) and effective electron mass $m_{e,\text{ox}}$ as shown in

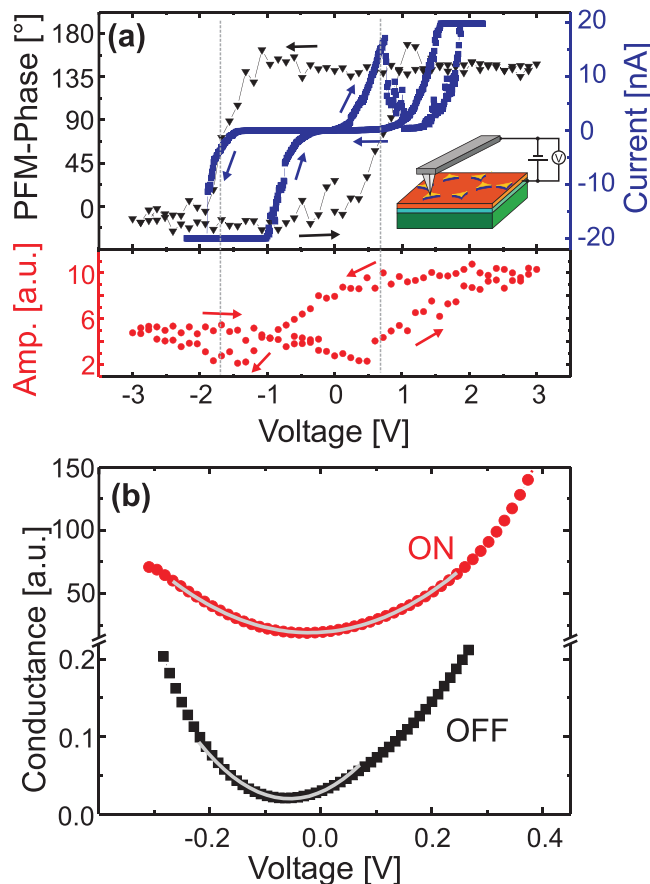


FIG. 2. (a) Current (■), PFM phase (▲), and PFM amplitude (●) signals measured on a Co/PZT(3 to 4 unit cells)/LSMO tunnel junction with an area of $0.04 \mu\text{m}^2$ as a function of an applied voltage. The direction of the voltage sweeps is given by the arrows. The measurement geometry is depicted in the inset. (b) Tunnel conductance as a function of voltage in the ON- (●) and OFF-state (■). The grey lines in (a) are to mark the coercive voltages and in (b) are fits to the Brinkman model.

TABLE I. Fit parameter to the Brinkman model obtained from the solid lines in Fig. 1(b).

State	d (nm)	$m_{e,\text{ox}}$ [m_e]	Φ_1 (eV)	Φ_2 (eV)
ON	1.6	3	0.65	0.7
OFF	1.6	6	0.44	0.59

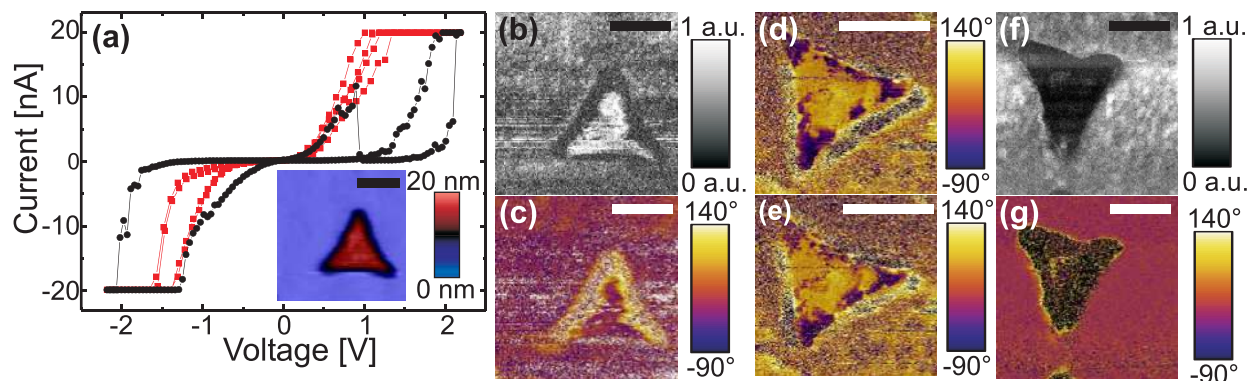


FIG. 3. (a) Current versus applied voltage in a switchable (●) and a non-switchable (■) Co/PZT(3 to 4 unit cells)/LSMO tunnel junction with an area of $0.04 \mu\text{m}^2$ each. The inset shows an AFM topography image of a typical junction. (b) PFM amplitude and (c) PFM phase images of the junction presented in the inset of (a). The low signal at the edges can be attributed to a bad mechanical and/or electrical contact between tip and electrode surface. (d) and (e) PFM phase images of another junction with a high PFM amplitude signal after applying (d) a -3 V and (e) a $+3 \text{ V}$ pulse to the Co electrode. Yellow (violet) depicts areas with polarization towards LSMO (Co). (f) PFM amplitude and (g) PFM phase images of a third type of a junction showing weak PFM response. All scale bars are 200 nm.

Table I. The change in $m_{e,ox}$ on polarization reversal can be explained on the basis of lattice strains³¹ or a polarization dependent complex band structure.¹² The present results are a direct experimental evidence of the influence of the ferroelectric polarization on the direct tunneling in ultra-thin ferroelectric barriers. This implicitly suggests a genuine electronic mechanism of resistive switching and TER in a ferroelectric tunnel junction.

Unfortunately, spontaneous backswitching from resistive ON- to OFF-state occurs rather fast, i.e., within several tens of seconds, as observed from the current relaxation (not shown here). This effect is likely due to polarization backswitching which in turn could be a result of large imprint of about 250 kV/mm revealed by the PFM-hysteresis (Fig. 2(a)). Moreover, not all junctions show resistive switching. Some junctions remain in the ON-state even after application of a large positive bias (Fig. 3(a)). Such a non-switchable ON-state can be explained by a pinned polarization state with polarization pointing towards LSMO. Similarly, a pinned polarization state may also lead to a non-switchable OFF-state for polarization pinned towards Co. To gain insight in this behavior, we have performed PFM imaging of tunnel junctions to reveal the domain structure underneath the top electrodes. There are basically three different types of junctions (Figs. 3(b)–3(g)). Two types, which exhibit high PFM amplitude signal, have polarization pointing towards either Co or LSMO, as concluded from the PFM phase contrast in Figs. 3(c) and 3(d). The polarization states in these junctions cannot be permanently switched by voltage pulses (Figs. 3(d) and 3(e)) because of the large imprint and corresponding backswitching of polarization during the PFM scan (several minutes).

In an extreme case, some junctions show low or zero PFM-amplitude and a noisy PFM-phase (Figs. 3(f) and 3(g)). On those devices, the ferroelectric behavior is suppressed most probably by defects in the PZT layer.³² In this case, the current would be high because a paraelectric barrier yields a higher conductivity than a ferroelectric barrier.³³ This high non-uniformity can be charged to the growth of the top Co electrodes which is an *ex situ* process. Different Co/PZT-interface quality across the sample might result in different preferred polarization states or even inferior Co/PZT-inter-

face quality. Additionally, a small difference in PZT thickness might induce as quite a strong difference in behavior. This is especially severe near the critical ferroelectric thickness as it is in the present case.

In summary, Co/PZT/LSMO ferroelectric tunnel junctions with PZT layers of only 3 to 4 unit cells thickness have been fabricated. Ferroelectric switching in the PZT layers has been demonstrated by PFM. The tunnel junctions show TER at room temperature with an ON/OFF ratio of about 300. The TER effect takes place only upon ferroelectric switching, and the ferroelectric coercive voltage and the voltage at which the resistance switches correlate within an experimental error. This provides direct experimental evidence of the effect of the ferroelectric polarization on direct tunneling in FTJs. Fitting of the experimental data by the Brinkman model yielded reasonable values for energy barrier height. The interface quality seems to play a crucial role in electronic processes in ferroelectric tunnel junctions and an *in-situ* structure monitoring of both metal-ferroelectric interfaces will be advantageous for optimizing the FTJ performance.

This work has been partly supported by DFG via SFB 762 and by EU project IFOX. D.P., A.G., and M.A. would like to acknowledge the support of the Leverhulme Trust for international network funding (F/00 203/V). D.H. and M.A. thank Norbert Schammelt and Mareike Herrmann for technical support. Work at the University of Nebraska was supported by the National Science Foundation (NSF) through Materials Research Science and Engineering Center (NSF Grant No. 0820521) and by the U.S. Department of Energy, Office of Basic Energy Sciences, Division of Materials Sciences and Engineering (DOE Grant DE-SC0004876).

¹J. F. Scott, *Ferroelectric Memories* (Springer, Berlin, 2000).

²L. Esaki, R. B. Laibowitz, and P. J. Stiles, *IBM Tech. Discl. Bull.* **13**, 2161 (1971).

³J. R. Contreras, H. Kohlstedt, U. Poppe, R. Waser, C. Buchal, and N. A. Pertsev, *Appl. Phys. Lett.* **83**, 4595 (2003).

⁴H. Kohlstedt, A. Petraru, K. Szot, A. Rüdiger, P. Meuffels, H. Haselier, R. Waser, and V. Nagarajan, *Appl. Phys. Lett.* **92**, 062907 (2008).

⁵V. Garcia, S. Fusil, K. Bouzouhane, S. Enouz-Vedrenne, N. D. Mathur, A. Barthélémy, and M. Bibes, *Nature (London)* **460**, 81 (2009).

- ⁶A. Crassous, V. Garcia, K. Bouzouane, S. Fusil, A. H. G. Vlooswijk, G. Rispens, B. Noheda, M. Bibes, and A. Barthélémy, *Appl. Phys. Lett.* **96**, 042901 (2010).
- ⁷D. Pantel, S. Goetze, D. Hesse, and M. Alexe, *ACS Nano* **5**, 6032 (2011).
- ⁸A. Q. Jiang, C. Wang, K. J. Jin, X. B. Liu, J. F. Scott, C. S. Hwang, T. A. Tang, H. B. Liu, and G. Z. Yang, *Adv. Mater.* **23**, 1277 (2011).
- ⁹P. Maksymovych, S. Jesse, P. Yu, R. Ramesh, A. P. Baddorf, and S. V. Kalinin, *Science* **324**, 1421 (2009).
- ¹⁰A. Gruverman, D. Wu, H. Lu, Y. Wang, H. W. Jang, C. M. Folkman, M. Y. Zhuravlev, D. Felker, M. Rzechowski, C. B. Eom, and E. Y. Tsymbal, *Nano Lett.* **9**, 3539 (2009).
- ¹¹A. Bune, S. Ducharme, V. Fridkin, L. Blinov, S. Palto, N. Petukhova, and S. Yudin, *Appl. Phys. Lett.* **67**, 3975 (1995).
- ¹²A. Chanthbouala, A. Crassous, V. Garcia, K. Bouzouane, S. Fusil, X. Moya, J. Allibe, B. Dlubak, J. Grollier, S. Xavier, C. Deranlot, A. Moshar, R. Proksch, N. D. Mathur, M. Bibes, and A. Barthélémy, *Nat. Nanotechnol.* **7**, 101 (2011).
- ¹³R. Waser, R. Dittmann, G. Staikov, and K. Szot, *Adv. Mater.* **21**, 2632 (2009).
- ¹⁴S. Kalinin, S. Jesse, A. Tselev, A. P. Baddorf, and N. Balke, *ACS Nano* **5**, 5683 (2011).
- ¹⁵D. Pantel and M. Alexe, *Phys. Rev. B* **82**, 134105 (2010).
- ¹⁶E. Y. Tsymbal and H. Kohlstedt, *Science* **313**, 181–183 (2006).
- ¹⁷V. Garcia, M. Bibes, L. Bocher, S. Valencia, F. Kronast, A. Crassous, X. Moya, S. Enouz-Vedrenne, A. Gloter, D. Imhoff, C. Deranlot, N. D. Mathur, S. Fusil, K. Bouzouane, and A. Barthélémy, *Science* **327**, 1106 (2010).
- ¹⁸M. Hambe, A. Petraru, N. A. Pertsev, P. Munroe, V. Nagarajan, and H. Kohlstedt, *Adv. Funct. Mater.* **20**, 2436 (2010).
- ¹⁹J. P. Velev, C.-G. Duan, J. D. Burton, A. Smogunov, M. K. Niranjan, E. Tosatti, S. S. Jaswal, and E. Y. Tsymbal, *Nano Lett.* **9**, 427 (2009).
- ²⁰D. Pantel, S. Goetze, D. Hesse, and M. Alexe, *Nat. Mater.* **11**, 289–293 (2012).
- ²¹M. Y. Zhuravlev, S. S. Jaswal, E. Y. Tsymbal, and R. F. Sabirianov, *Appl. Phys. Lett.* **87**, 222114 (2005).
- ²²M. Y. Zhuravlev, R. F. Sabirianov, S. S. Jaswal, and E. Y. Tsymbal, *Phys. Rev. Lett.* **94**, 246802 (2005).
- ²³I. Vrejoiu, G. Le Rhun, L. Pintilie, D. Hesse, M. Alexe, and U. Gösele, *Adv. Mater.* **18**, 1657 (2006).
- ²⁴B. J. Rodriguez, C. Callahan, S. V. Kalinin, and R. Proksch, *Nanotechnology* **18**, 475504 (2007).
- ²⁵P. Ghosez and K. M. Rabe, *Appl. Phys. Lett.* **76**, 2767 (2000).
- ²⁶H. F. Kay and J. W. Dunn, *Philos. Mag.* **7**, 2027 (1962).
- ²⁷X. Hong, A. Posadas, and C. H. Ahn, *Appl. Phys. Lett.* **86**, 142501 (2005).
- ²⁸J. Kötzler and W. Gil, *Phys. Rev. B* **72**, 060412 (2005).
- ²⁹J. J. Åkerman, J. M. Slaughter, R. W. Dave, and I. K. Schuller, *Appl. Phys. Lett.* **79**, 3104 (2001).
- ³⁰W. F. Brinkman, R. C. Dynes, and J. M. Rowell, *J. Appl. Phys.* **41**, 1915 (1970).
- ³¹H. Kohlstedt, N. A. Pertsev, J. R. Contreras, and R. Waser, *Phys. Rev. B* **72**, 125341 (2005).
- ³²M.-W. Chu, I. Szafraniak, R. Scholz, C. Harnagea, D. Hesse, M. Alexe, and U. Gösele, *Nat. Mater.* **3**, 87 (2004).
- ³³J. P. Velev, C.-G. Duan, K. D. Belashchenko, S. S. Jaswal, and E. Y. Tsymbal, *Phys. Rev. Lett.* **98**, 137201 (2007).